High Resolution TEM
without and with Cs corrected microscopes

- K. Ishizuka (1980) ***"Contrast Transfer of Crystal Images in TEM"***, Ultramicroscopy **5**,pages 55-65.
- L. Reimer (1993) ***"Transmission Electron Microscopy"***, Springer Verlag, Berlin.
- J.C.H. Spence (1988), ***"Experimental High Resolution Electron Microscopy"***, Oxford University Press, New York.

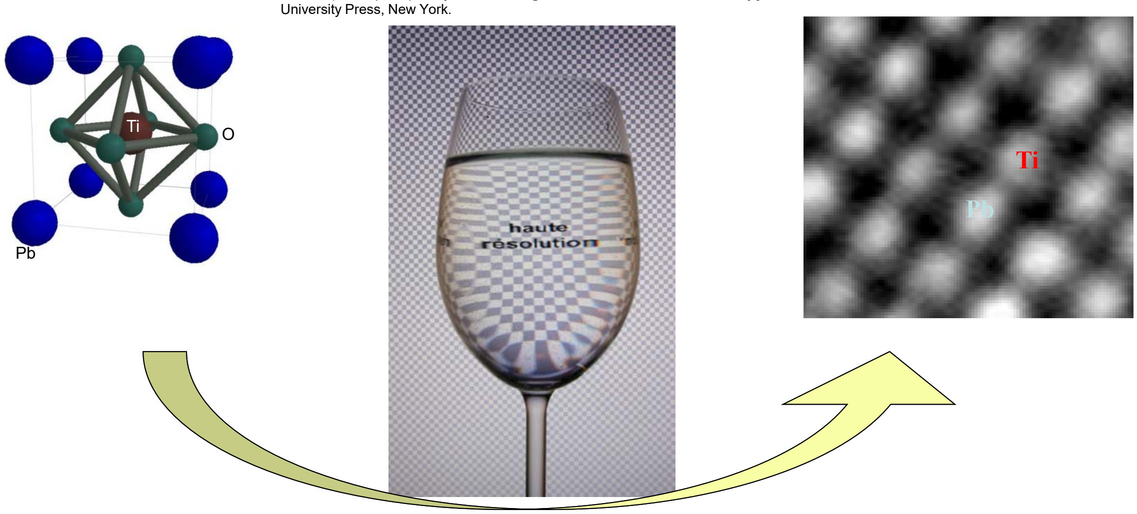

Abbé's principle in light optics

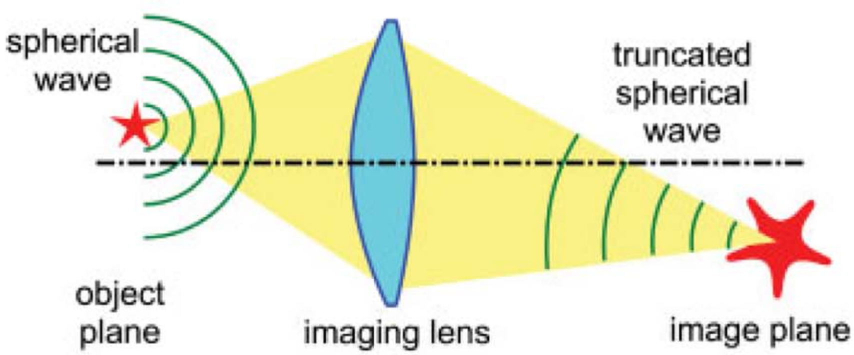

Figure 21-2: Image formation of self-luminous objects.

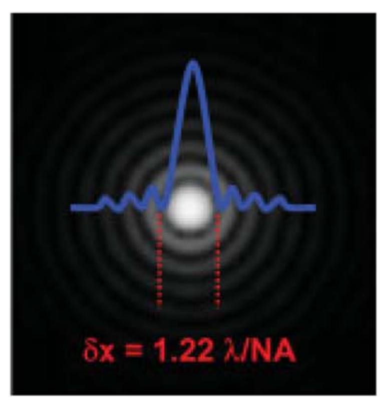

x: resolution (point spread function)
λ: wave length
NA: numerical aperture (lens diameter)

Handbook of Optical Systems: Vol. 2. Physical Image Formation.

Abbé: image formation by diffraction

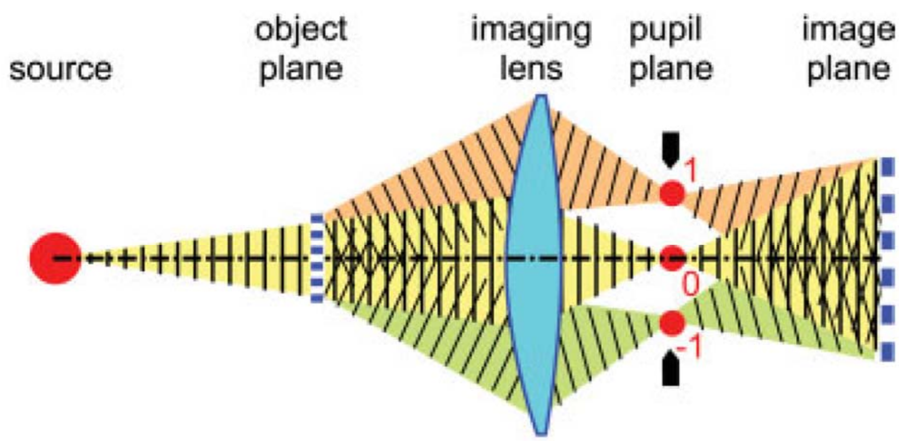

Figure 21-3: Abbe Theory of image formation by diffraction and interference.

Abbé's principle of image formation

A lens is an analogous «light-speed fast» Fourier-Transformer

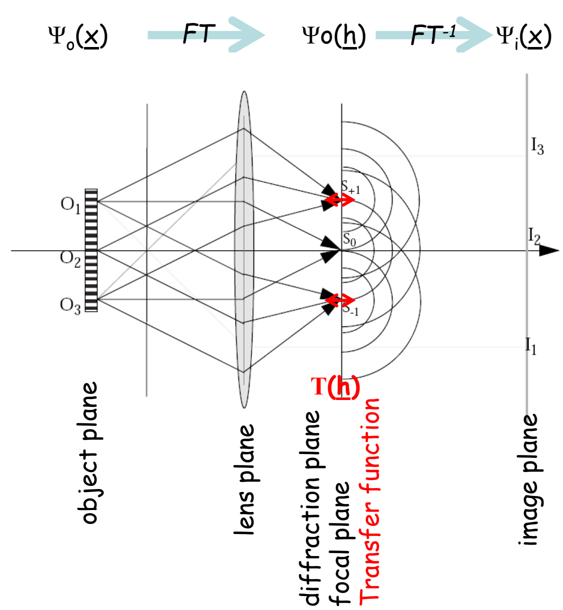

Abbé's principle mathematically

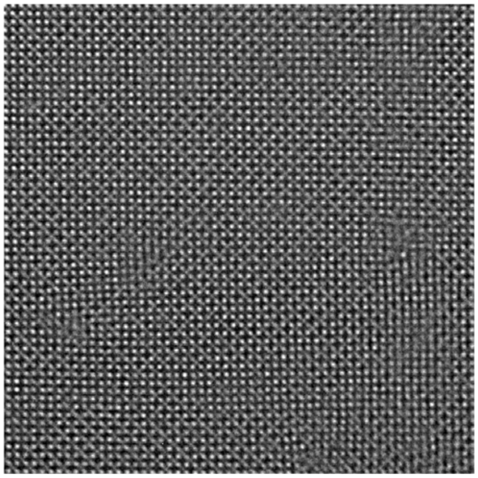

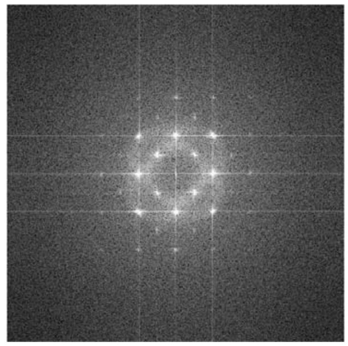

FFT

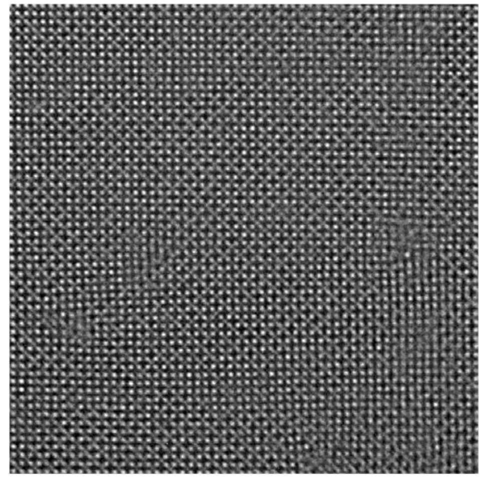

object $\xrightarrow{FT}$ $\xrightarrow{FT^{-1}}$ image

Abbé's principle mathematically

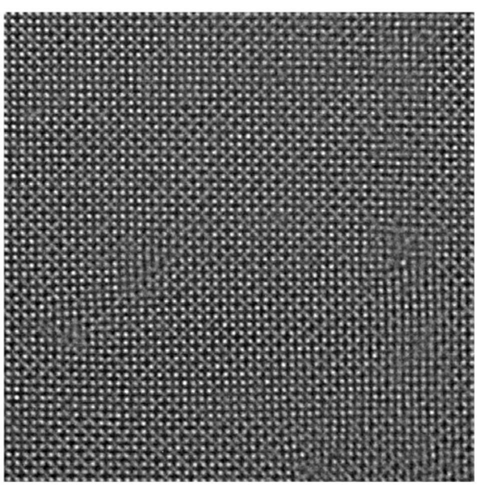

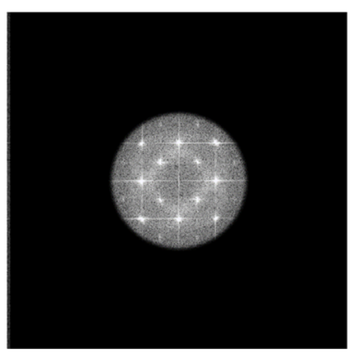

FFT

with mask

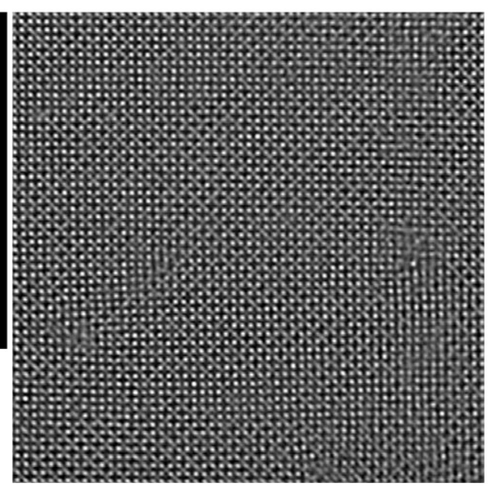

object $\xrightarrow{FT}$ $\xrightarrow{FT^{-1}}$ image

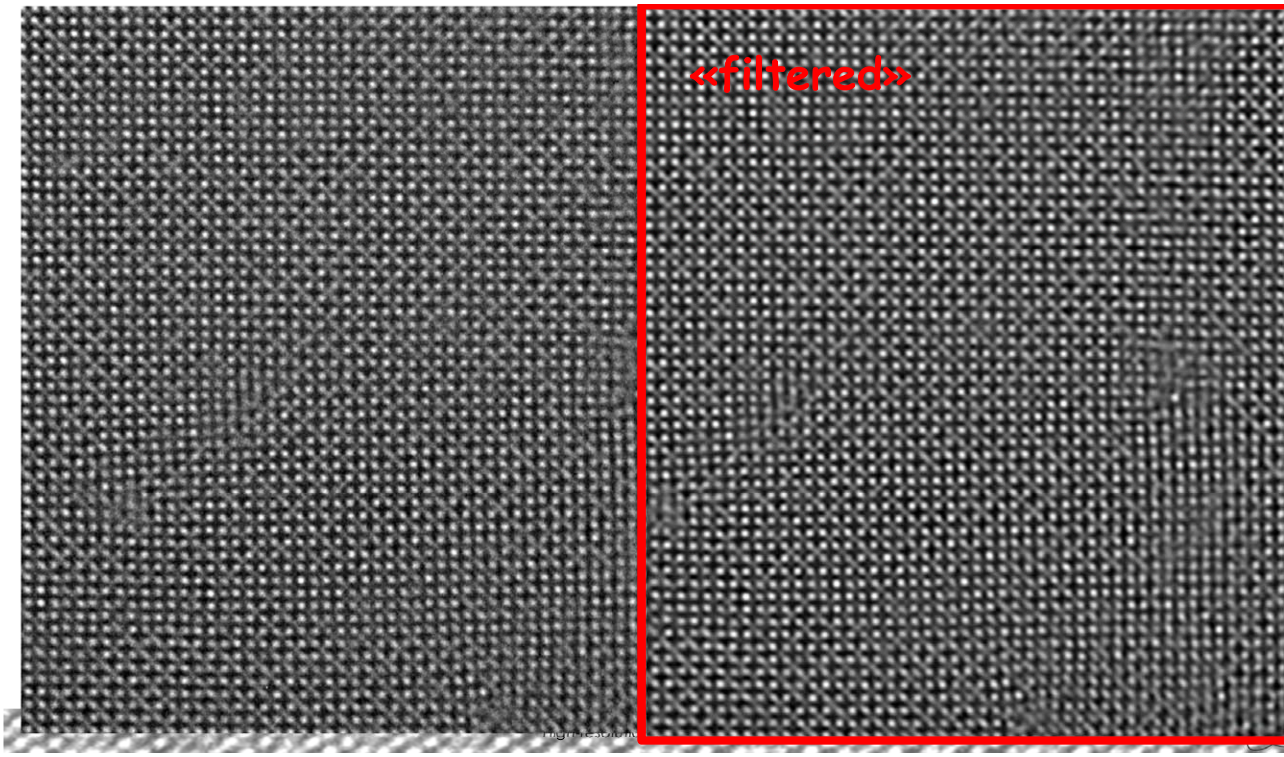

Abbé's principle mathematically

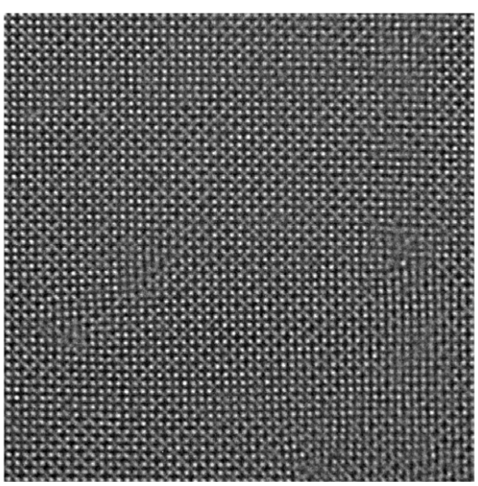

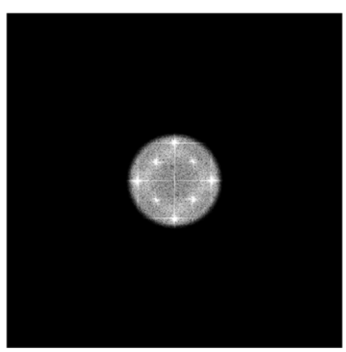

FFT

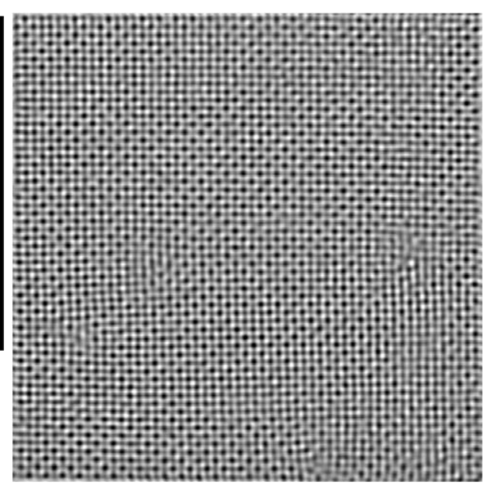

object $\xrightarrow{FT}$ $\xrightarrow{FT^{-1}}$ image

Abbé's principle mathematically

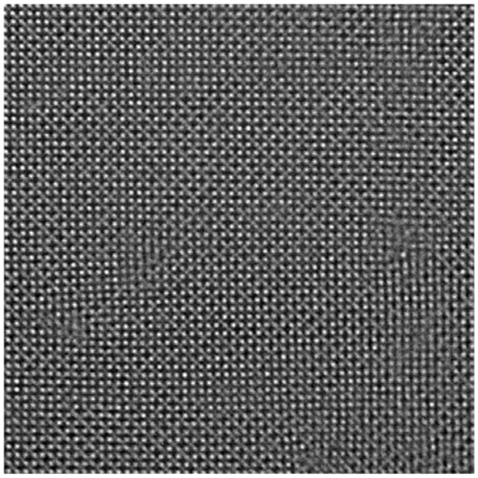

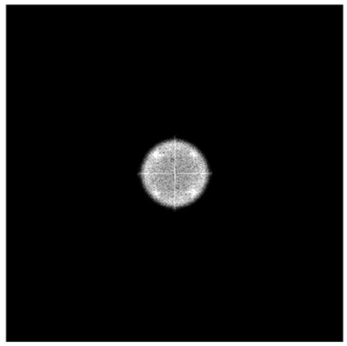

FFT

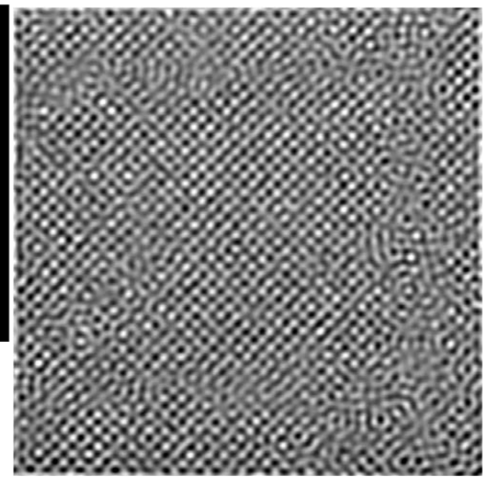

object $\xrightarrow{FT}$ $\xrightarrow{FT^{-1}}$ image

Abbé's principle mathematically

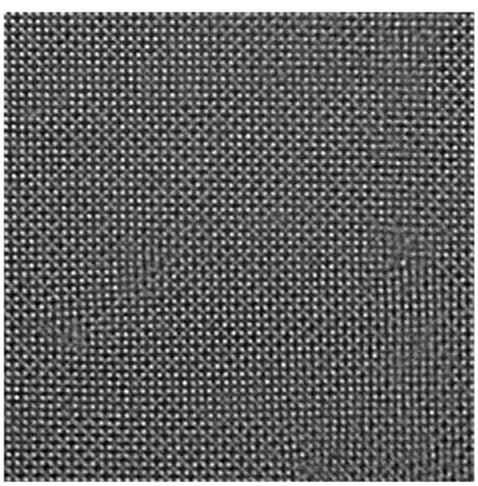

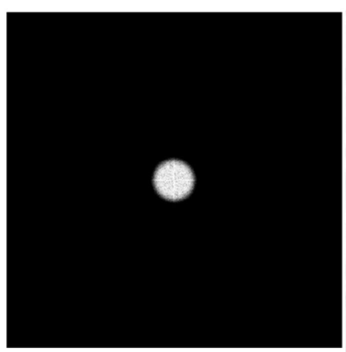

FFT

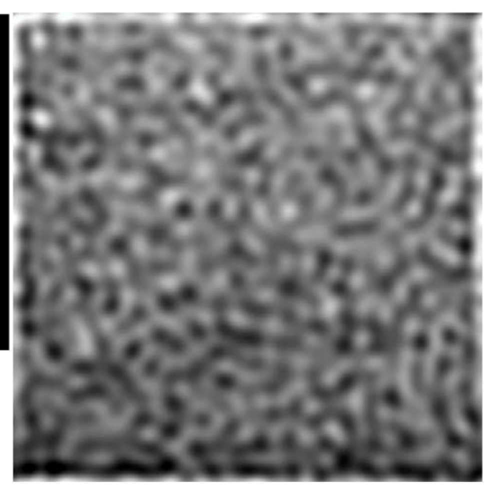

object $\xrightarrow{FT}$ $\xrightarrow{FT^{-1}}$ image

the TEM in “high-resolution” mode

A high-resolution image is an interference image of the transmitted and the diffracted beams!

Diffracted electrons: coherent elastic scattering
(the electrons have seen the crystal lattice)

The quality of the image depends on the optical system that makes the beams interfere

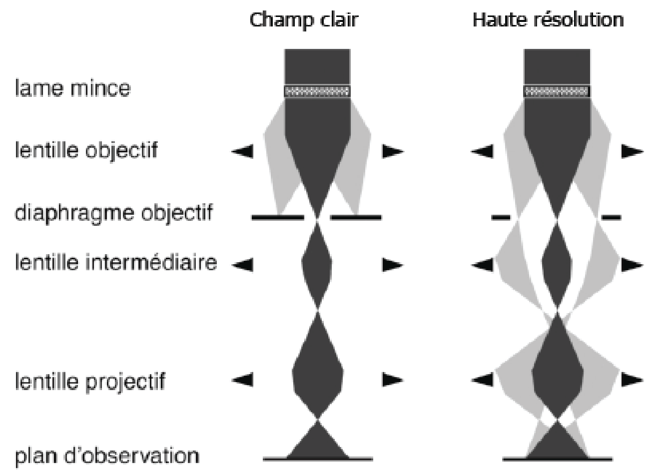

Bright Field High-Resolution

High-resolution

Expectation: The image should resemble the atomic structure !

Atoms…?
Thin samples: atom columns: orientation of the sample (incident beam // atom columns)

The observed contrast varies with thickness and defocalisation…!

Need to compare with simulations !

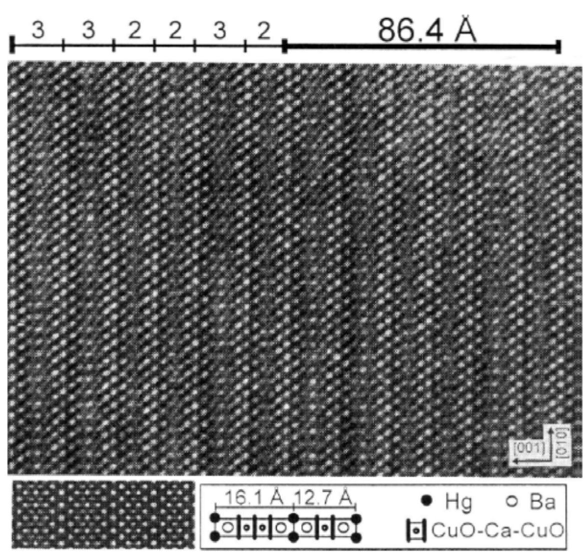

the objective lens

Field with rotational symmetry

Lorentz Force : **F** = -e **v** ^ **B**

e on optical axis: **F** = 0, e not on optical axis : deviated

optical axis: symmetry axis

Scherzer 1936:

Magnetic lens with **rotational symmetry**:

Aberration coefficients:

C_s: spherical

C_c: chromatical

Always positive !!

$$C_s = \frac{1}{16}\int_{z_o}^{z_i}\left\{b^4h^4 + 2\left(hb' + h'b\right)^2 h^2 + 2b^2h^2h'^2\right\}dz$$

$$C_c = \frac{1}{4}\int_{z_o}^{z_i} b^2h^2 dz$$

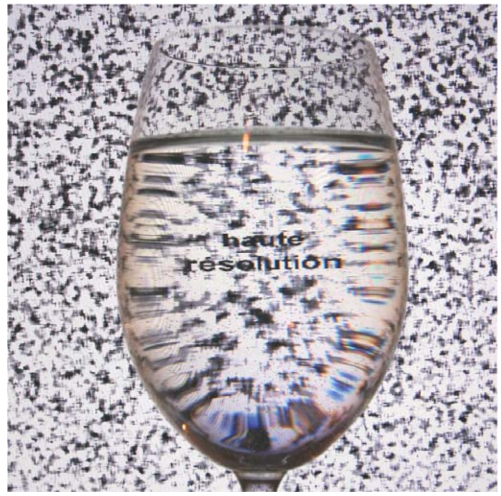

« Scherzer » resolution limit: $D_{res} = 0.66\lambda^{3/4}C_s^{\ 1/4}$

Example: Talos/Osiris

λ= 0.00197nm, C_s = 1.8 mm

D_{res} = 2.2 10^{-10} = 2.2Å

Image formation

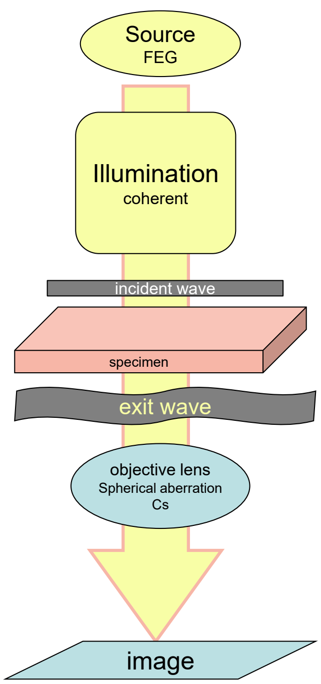

- **Source:** *coherent and monochromatic*
- **Illumination:** *parallel*
- **Sample:** thin, *nicely prepared (no amorphization), orientation (zone axis)*
- **objective lens:** *aberrations, focus, stability !*
- **projection** lens system *(magnification)*

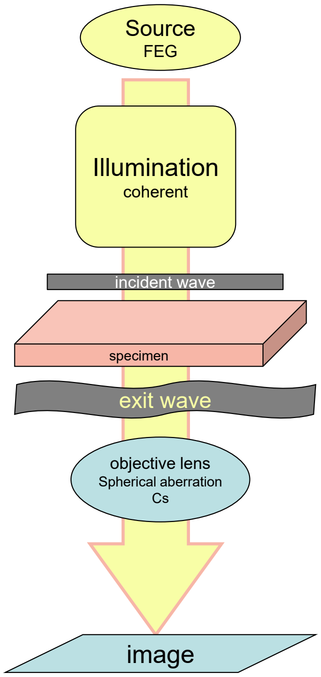

Image formation

- **Illumination:** *parallel beam* $\Psi(\vec{\mathbf{r}}) = \Psi_0 \exp^{2\pi i \vec{\mathbf{k}}\cdot\vec{\mathbf{r}}}$
- **Sample:**

  weak phase object:
  weak phase object aproximation (WPOA)
- **Objective lens:**

  Abbé's principle
  transfert function
  coherent transfer function (CTF)

  $$\Psi_i(\vec{\mathbf{x}}) = \Psi_o(\vec{\mathbf{x}}) \otimes T(\vec{\mathbf{x}})$$
- **Image contrast** (intensity) $\mathrm{I}_i(\vec{\mathbf{x}}) = \Psi_i(\vec{\mathbf{x}})\Psi_i^*(\vec{\mathbf{x}})$

elastic scattering
sample = pure phase objet

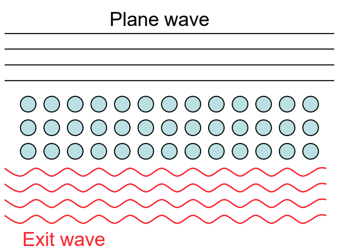

Cristal potential

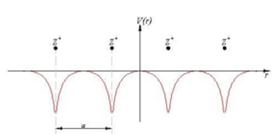

Cristal potential = phase object

Wave vector in vacuum:

$$k = \sqrt{2me(E) \big/ h^2}$$

Wave vector in a potential:

$$k = \sqrt{2me(E + V(\vec{r})) \big/ h^2}$$

Phase shift $\Delta\alpha$ due to the cristal potential V_p:

$$\Delta\alpha = \frac{\sigma}{2\pi} V_p(\vec{x}, z)$$

$$\sigma = \pi \big/ \lambda E$$

Exit wave function: $\Psi_o(\vec{\mathbf{x}}) = exp\left[-i\sigma V_p(\vec{\mathbf{x}}; z)\right]$

Transfer Function

The optical system (lenses) can be described by a convolution with a transfer function T(x):
Point spread function (PSF): describes how a point on the object side is transformed into the image.

$$\Psi_i(\underline{x}) = \int_{-\infty}^{\infty} \Psi_o(\underline{u}) T(\underline{x}-\underline{u}) d\underline{u} = \Psi_o(\underline{x}) \otimes T(\underline{x})$$

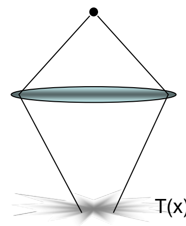

- ***Transfer Function***:
  describe how a complex“object” wave-function is transfered into an “image” wave-function

$$\Psi_i(\underline{h}) = \Psi_o(\underline{h}) T(\underline{h})$$

- **The image INTENSITY** observed on a screen (or a camera / negative plate etc.)

$$I_i(\underline{x}) = \Psi_i(\underline{x}) \Psi_i^*(\underline{x}) \qquad I_i(\underline{h}) = \Psi_i(\underline{h}) \otimes \Psi_i^*(-\underline{h}) = \int \Psi_i(\underline{h}') \Psi_i^*(\underline{h}-\underline{h}') d\underline{h}'$$

$$I_i(\underline{h}) = [\Psi_o(\underline{h}) T(\underline{h})] \otimes [\Psi_o^*(-\underline{h}) T^*(-\underline{h})]$$

Transfer Function

$$T(\vec{\mathbf{h}}) = a(\vec{\mathbf{h}}) \exp\left[2\pi i \chi(\vec{\mathbf{h}})\right] E_s(\vec{\mathbf{h}}) E_t(\vec{\mathbf{h}})$$

- Phase factors:
  - Spherical Aberration
  - Defocus
- Amplitude factors:
  - (objective) apertures
  - spatial coherence enveloppe (non-parallel, convergent beam)
  - Temporal coherence envelope (non monochromatic beam, instabilities of the gun and lenses)

Transfer Function

$$T(\vec{\mathbf{h}}) = \exp\left[2\pi i\chi(\vec{\mathbf{h}})\right]$$

$$\chi(\vec{\mathbf{h}}) = 0.25C_s\lambda^3h^4 + 0.5\Delta z\lambda h^2$$

Spherical aberration ← $0.25C_s\lambda^3h^4$; $0.5\Delta z\lambda h^2$ → defocus

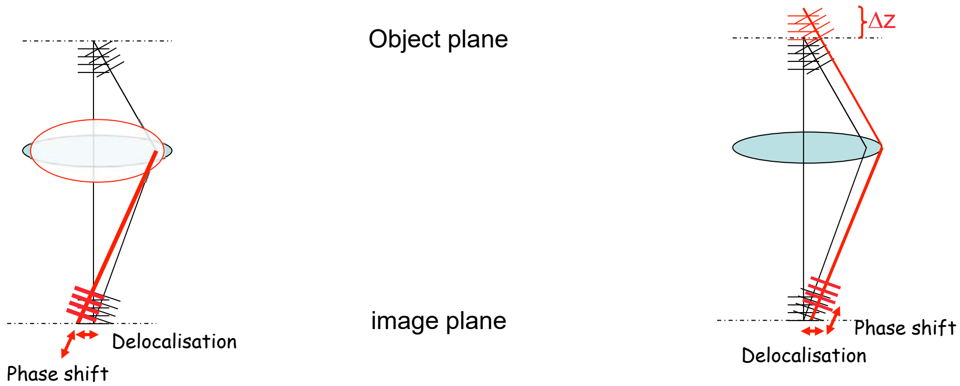

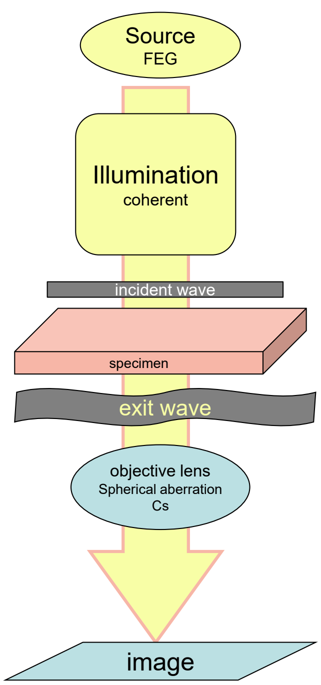

Image formation

- Illumination

$$\Psi(\vec{\mathbf{r}}) = \Psi_0 \exp^{2\pi i\vec{\mathbf{k}}\cdot\vec{\mathbf{r}}}$$

- Sample

$$\Psi_o(\vec{\mathbf{x}}) = exp\left[-i\sigma V_p(\vec{\mathbf{x}};z)\right] \cong 1 - i\sigma V_p(\vec{\mathbf{x}};z)$$

- objective lens

$$T(\vec{\mathbf{h}}) = \exp\left[2\pi i\chi(\vec{\mathbf{h}})\right] \quad avec \quad \chi(\vec{\mathbf{h}}) = 0.25C_s\lambda^3h^4 + 0.5\Delta z\lambda h^2$$

$$\Psi_i(\vec{\mathbf{x}}) = \Psi_o(\vec{\mathbf{x}}) \otimes T(\vec{\mathbf{x}})$$

- Image, contrast

$$\mathrm{I_i}(\vec{\mathbf{x}}) = \Psi_i(\vec{\mathbf{x}})\Psi_i^*(\vec{\mathbf{x}})$$

The « magic » of image contrast

Weak phase object

$$\Psi_o(\underline{x}) = exp[-i\sigma V_p(\underline{x};z)] \cong 1 - i\sigma V_p(\underline{x};z)$$

$$\left.\begin{aligned}\Psi_o(\underline{h}) &= \delta(\underline{h}) - i\sigma V_p(\underline{h})\\ \Psi_i(\underline{h}) &= \Psi_o(\underline{h})T(\underline{h}) = \Psi_o(\underline{h})exp[2\pi i\chi(\underline{h})]\\ \Psi_i(\underline{h}) &= [\delta(\underline{h}) - i\sigma V_p(\underline{h})][\cos 2\pi\chi(\underline{h}) + i\sin 2\pi\chi(\underline{h})]\end{aligned}\right\}$$ ***Fourier Space***

Selecting $\sin[2\pi\chi(\mathbf{\underline{h}})] = -1$, $\cos[2\pi\chi(\mathbf{\underline{h}})] = 0$ ***for the strongest reflections*** $\underline{\boldsymbol{h}}$

Image wave function

$$\Psi_i(\underline{h}) = \delta(\underline{h}) - \sigma V_p(\underline{h})$$

The image intensity $\Psi_i(\underline{\mathbf{x}})\,\Psi_i^*(\underline{\mathbf{x}})$ ***is given by :***

Intensity of a weak phase objet in "direct" contrast

$$I(\underline{x}) = (1 - \sigma V_p(\underline{x}))(1 + \sigma V_p(\underline{x})) = \boxed{1 - 2\sigma V_p(\underline{x})} + O(\sigma^2 V_p^2(\underline{x}))$$

but….

Selecting $\sin[2\pi\chi(\mathbf{\underline{h}})] = 0$, $\cos[2\pi\chi(\mathbf{\underline{h}})] = 1$. ***for the strongest reflections*** $\underline{\boldsymbol{h}}$

Image wave function

$$\Psi_i(\underline{h}) = [\delta(\underline{h}) - i\sigma V_p(\underline{h})]$$

Intensity of a weak phase objet in "reversed" contrast

$$I(\underline{x}) = (1 - i\sigma V_p(\underline{x}))(1 + i\sigma V_p(\underline{x})) = \boxed{1 + \sigma^2 V_p^2(\underline{x})}$$

Intensity is proportional to the square of the projected potential V_p : Image interpretation in terms of atom columns becomes complicated….

For a direct and simple interpretation of the image contrast:
the imaginary part (sin) of the transfer function exp[$2\pi i\chi$(h)] should be ~-1

The only free parameter in the microscope is: the defocus Δz

CTF

- CTF: contrast transfer function (« useful part » = V_p)

$$T(\vec{\mathbf{h}}) = \exp\left[2\pi i \chi(\vec{\mathbf{h}})\right]$$
$$\chi(\vec{\mathbf{h}}) = 0.25 C_s \lambda^3 h^4 + 0.5 \Delta z \lambda h^2$$

$$CTF(h) = -\sin\left[\frac{\pi}{2} C_s \lambda^3 h^4 + \pi \Delta z \lambda h^2\right]$$

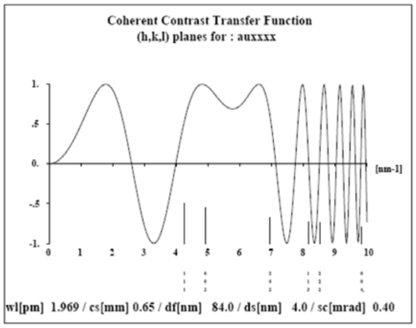

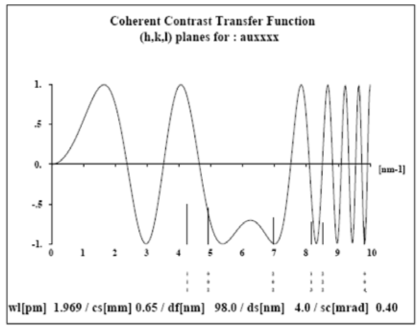

« Scherzer Defocus »

With $\Delta z_{scherzer}$

$$\Delta z = -\sqrt{{}^{4}/_{3}\, C_s \lambda}$$

The CTF has a wide pass band

$$D_{scherzer} = -0.66 \lambda^{3/4} C_s^{\ 1/4}$$

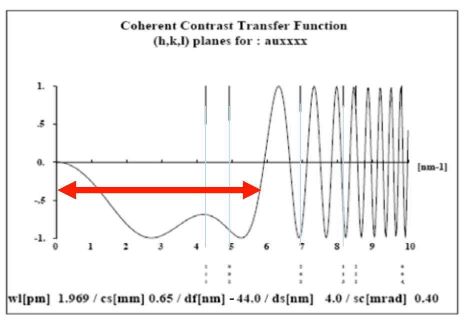

The first zero crossing of the CTF defines the « **point-to-point** » resolution of an electron microscope
The atom columns appear as dark areas on a bright background

$$I(\underline{x}) = (1 - \sigma V_p(\underline{x}))(1 + \sigma V_p(\underline{x})) = 1 - 2\sigma V_p(\underline{x}) + O(\sigma^2 V_p^2(\underline{x}))$$

Spatial and temporal coherence

$$T(\vec{\mathbf{h}}) = a(\vec{\mathbf{h}})\exp\left[2\pi i\chi(\vec{\mathbf{h}})\right]E_s(\vec{\mathbf{h}})E_t(\vec{\mathbf{h}})$$

Fluctuations of lens current
Fluctuations of High Tension

CM300UT FEG
Field emission
C_s: 0.7mm
Dz= -44nm

Resolution (point to point): 1.7Å
Information limit : ~1.2Å

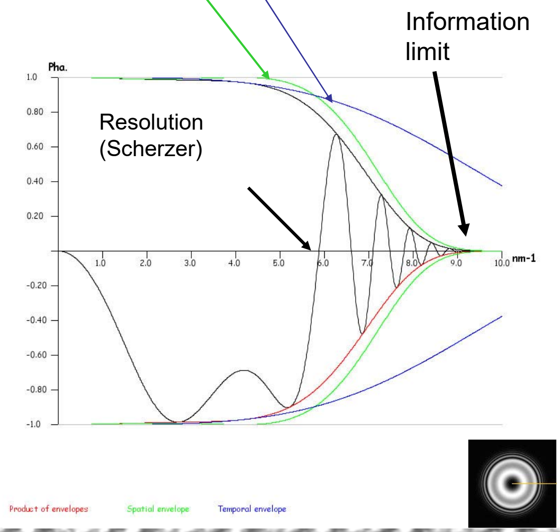

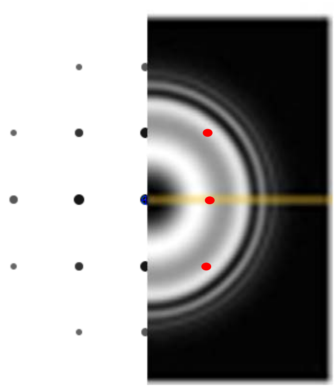

Back focal plane (diffraction plane)

Defocus

Wave funct.

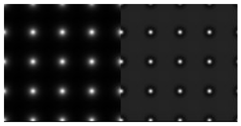

proj. pot.

defocus

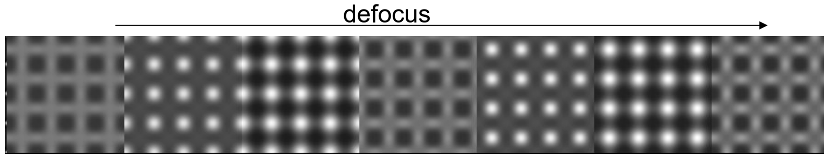

scherzer 1. p.b. 2. p.b.

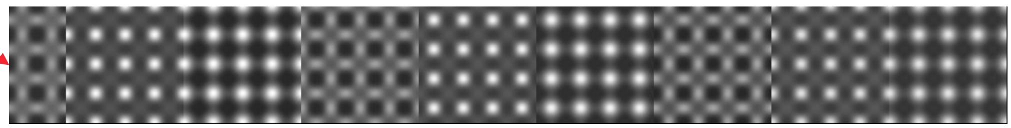

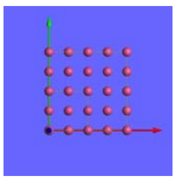

3. p.b.

Au [100], thickness 20nm

Pass bands

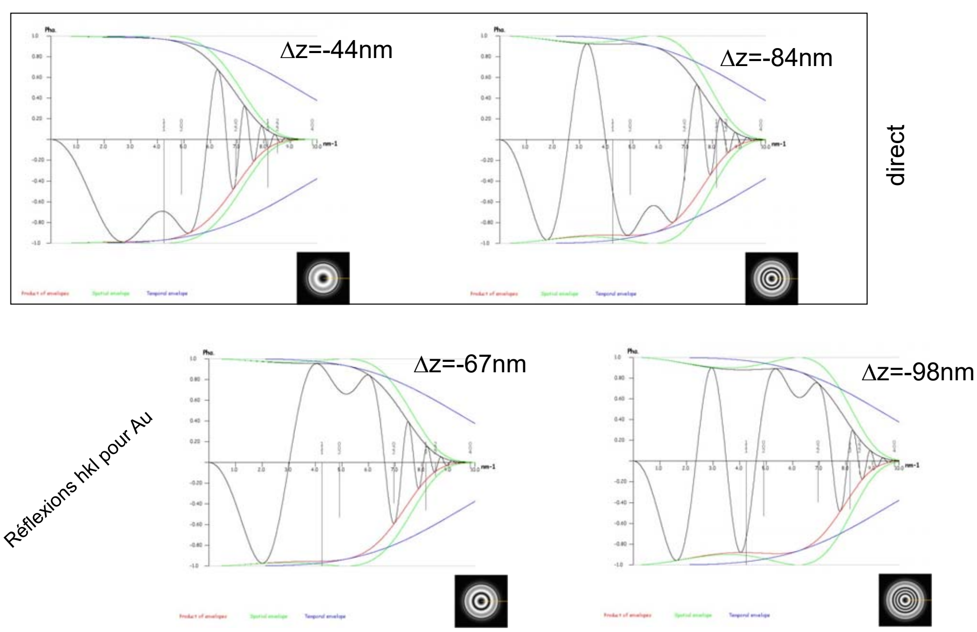

HRTEM image formation

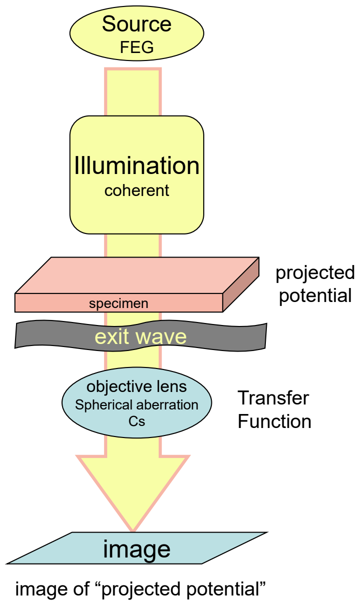

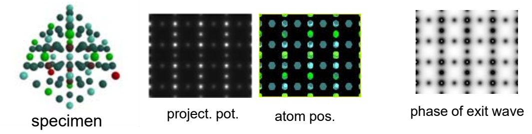

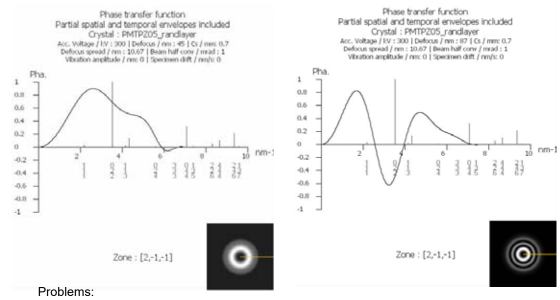

Problems:
defocusing for contrast: delocalization of information, information limit not used

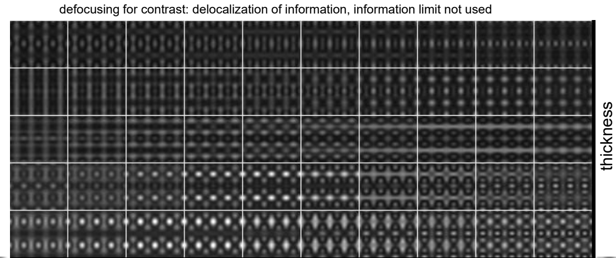

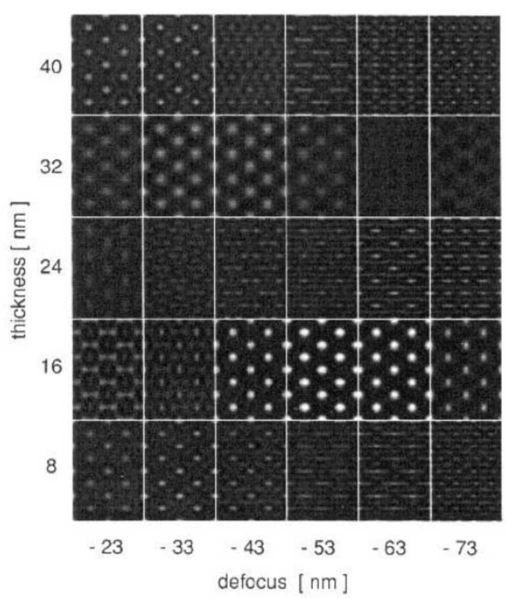

Thickness-defocus map in Fe3Al intermetallics
M. Karlik Materials structure, 8 (2001),3

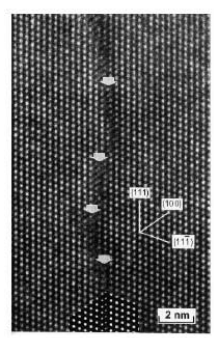

Experiment

What do you notice ?

Can you figure out the underlying explanation?

"delocalisation"

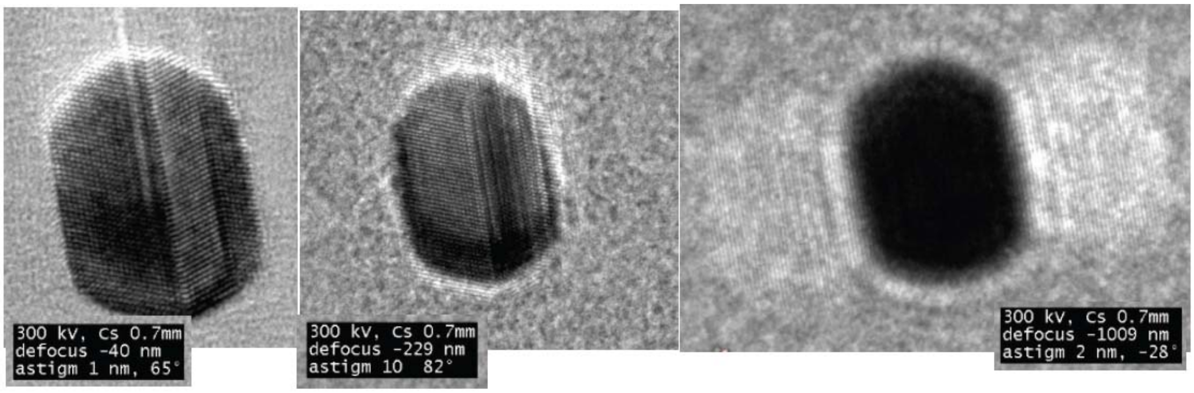

Au nanoparticle on amorphous carbon. Various defocalisation

Effect of defocus <-> «phantom images»

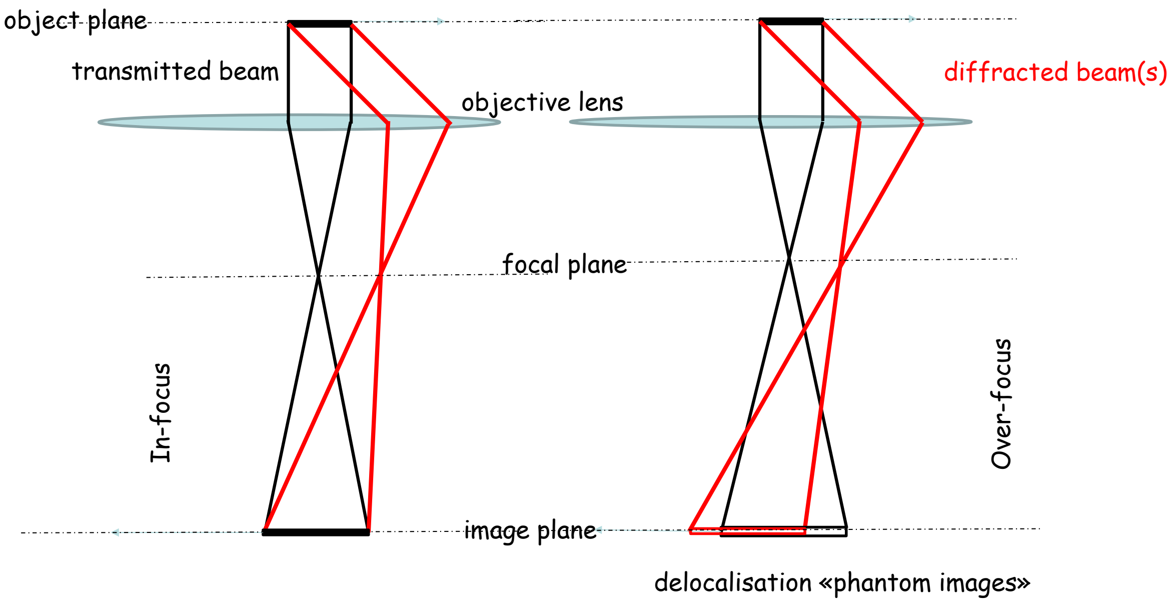

1 HRTEM examples from the Talos: imaging nanowire defects

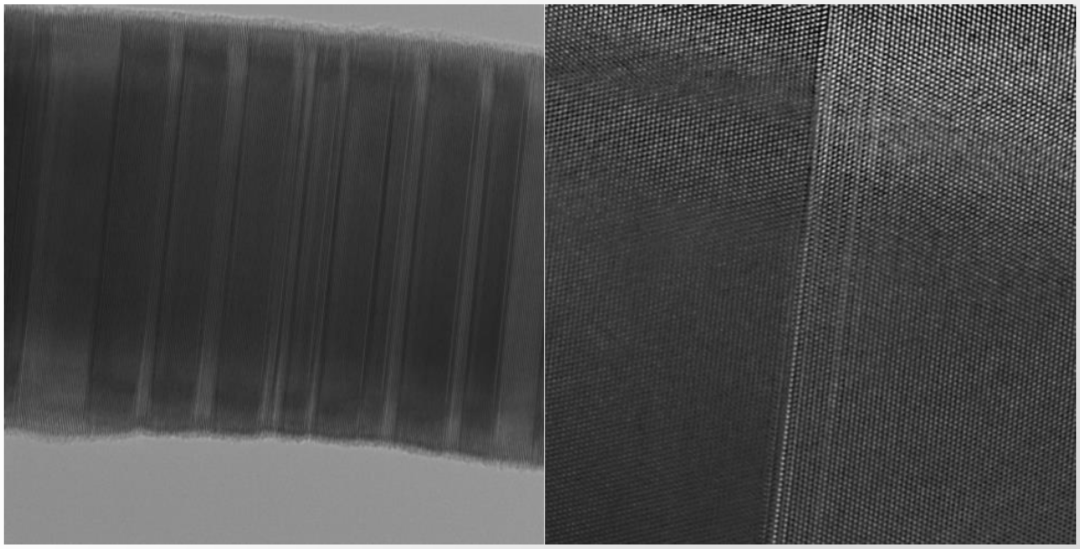

Can we see the effect of the transfer function…?

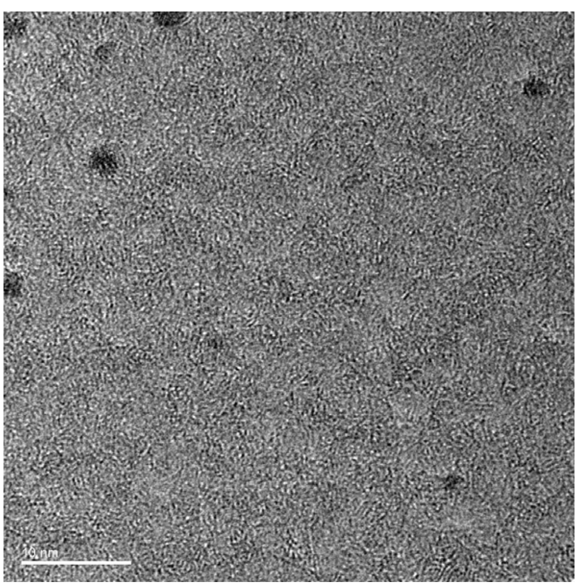

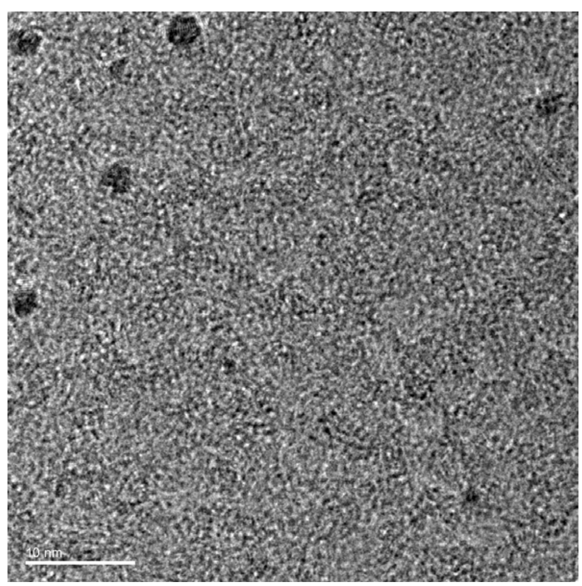

The FFT tells the «truth»

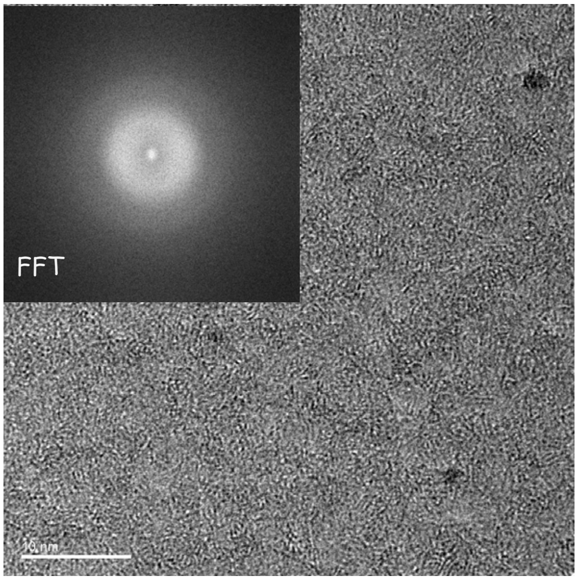

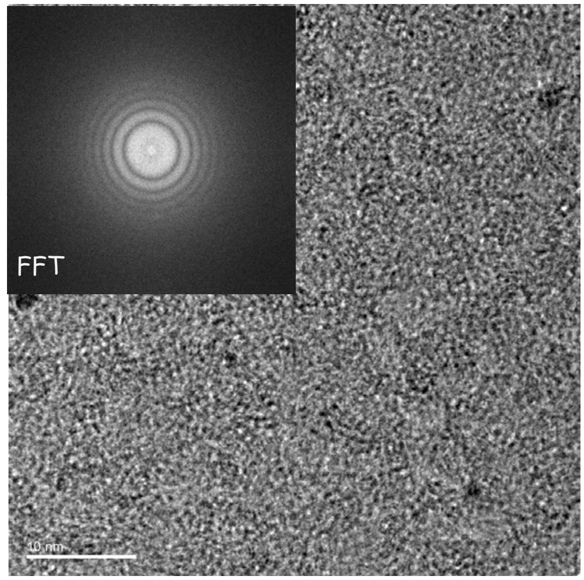

Astigmatism…

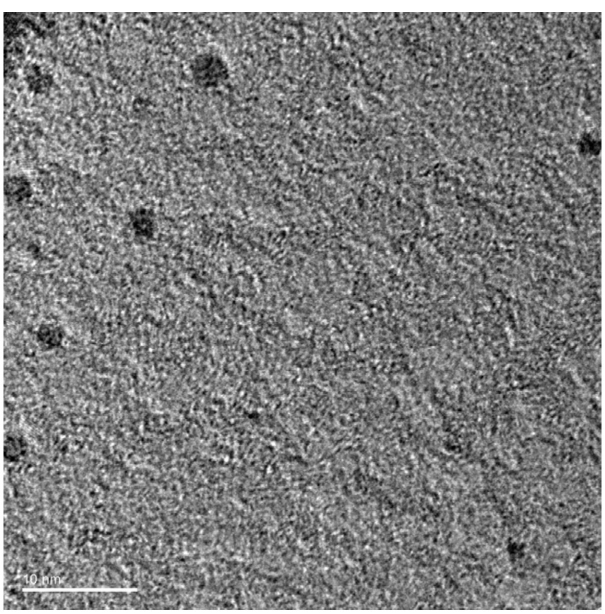

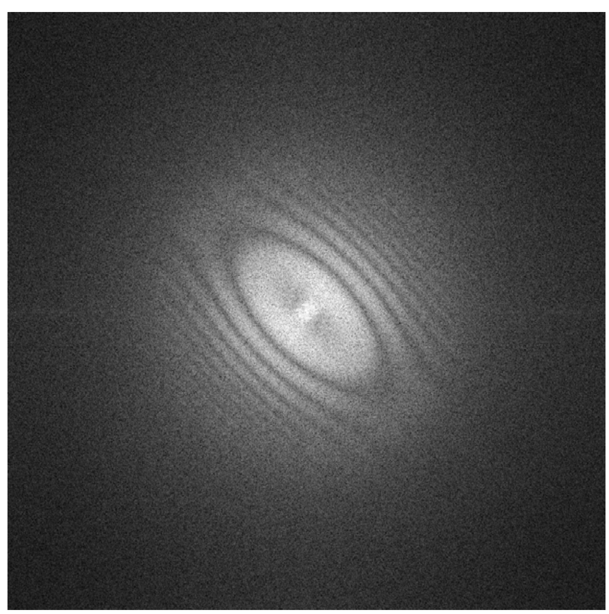

HRTEM image formation

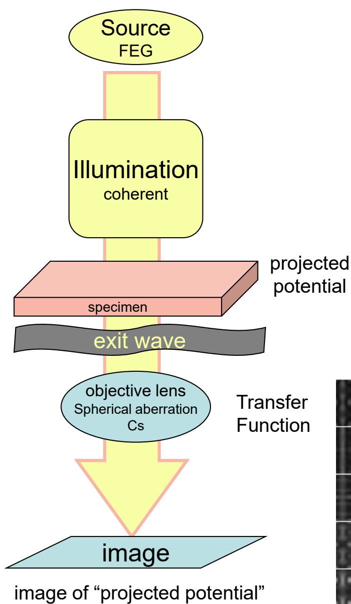

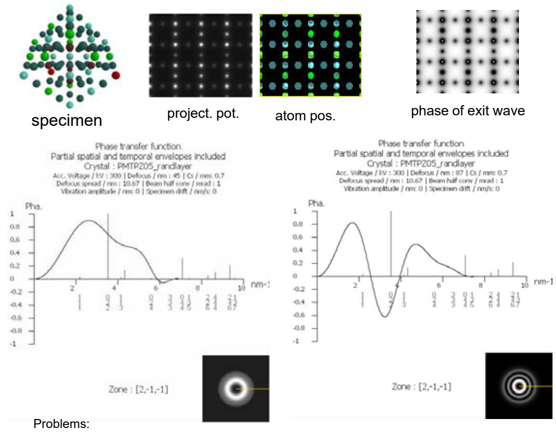

Problems:
defocusing for contrast: delocalization of information, information limit not used

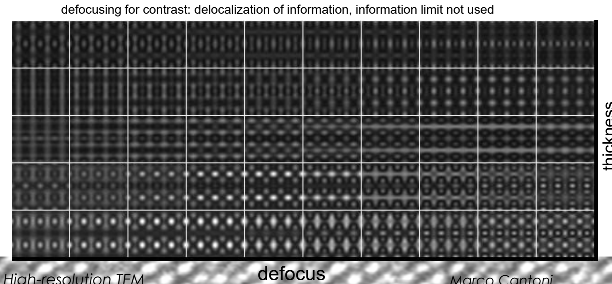

Aberration-Corrected Analytical Transmission Electron Microscopy, First Edition.
Edited by Rik Brydson.
© 2011 John Wiley & Sons, Ltd. Published 2011 by John Wiley & Sons, Ltd.

Table A.1 The name, order in **K** and azimuthal symmetry for the aberration coefficients.

Aberration Coefficient	Krivanek notation	Order in K	Azimuthal symmetry
Image shift	$C_{0,1}$	1	1
Two fold astigmatism	$C_{1,2}$	2	2
Defocus (over focus positive)	$C_{1,0}$	2	inf
Three fold astigmatism	$C_{2,3}$	3	3
Axial coma	$C_{2,1}$	3	1
Four fold astigmatism	$C_{3,4}$	4	4
Axial star aberration	$C_{3,2}$	4	2
Spherical aberration	$C_{3,0}$	4	inf
Five fold astigmatism	$C_{4,5}$	5	5
Fourth order axial coma	$C_{4,1}$	5	1
Three lobe aberration	$C_{4,3}$	5	3
Six fold astigmatism	$C_{5,6}$	6	6
Fifth order rosette aberration	$C_{5,4}$	6	4
Fifth order axial star aberration	$C_{5,2}$	6	2
Fifth order spherical aberration	$C_{5,0}$	6	inf
Seven fold astigmatism	$C_{6,7}$	7	7
Sixth order axial coma	$C_{6,1}$	7	1
Sixth order three lobe aberration	$C_{6,3}$	7	3
Sixth order pentacle aberration	$C_{6,5}$	7	5
Eight fold astigmatism	$C_{7,8}$	8	8
Seventh order hexagon aberration	$C_{7,6}$	8	6
Seventh order rosette aberration	$C_{7,4}$	8	4
Seventh order star aberration	$C_{7,2}$	8	2
Seventh order spherical aberration	$C_{7,0}$	8	inf

There is no generally accepted notation for the aberration coefficients. In this book we have used the notation of Krivanek *et al.* (1999) who distinguish the aberration coefficients by means of two subscripts, the first denoting the order of the aberration (in terms of the wavevector K) and the second, the (azimuthal) symmetry about the optic axis (as indicated in Table A.1 below). A further subscript label (a, b) is needed to separate orthogonal contributions to the same aberration when these are present.

Table A.2 The different notations for the aberration coefficients (this table includes terms not present in the publications cited, supplied by the authors in question – reproduced from Hawkes, 2008).

Uhlemann and Haider (1998)	Saxton (1995)	Krivanek *et al.* (1999)	Hawkes and Kasper (1989)
C_1	C_1	C_1	
A_1	A_1	$C_{1,2}$	$b_1 + ib_2$
B_2	$\frac{1}{3}\overline{B}_2$	$\frac{1}{3}C^*_{2,1}$	$\frac{1}{4}(3A_{30} - 3iA_{03} + A_{12} - iA_{21})$
A_2	A_2	$C_{2,3}$	$\frac{3}{4}(3A_{30} - 3iA_{03} + A_{12} - iA_{21})$
$C_s = C_3$	C_3	$C_{3,0} = C_3$	
S_3	$\frac{1}{4}\overline{B}_3$	$\frac{1}{4}C^*_{3,2}$	
A_3	A_3	$C_{3,4}$	
B_4		$\frac{1}{5}C^*_{4,1}$	
D_4		$\frac{1}{5}C^*_{4,3}$	
A_4		$C_{4,5}$	
C_5		$C_{5,0} = C_5$	
S_5		$\frac{1}{6}C^*_{5,2}$	
A_5		$C_{5,6}$	
R_5		$\frac{1}{6}C^*_{5,4}$	

From https://www.globalsino.com/EM/page3740.html

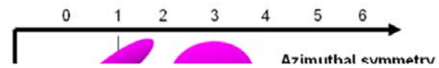

Transfer Function

$$T(\vec{\mathbf{h}}) = \exp\left[2\pi i \chi(\vec{\mathbf{h}})\right]$$

$$\chi(\vec{\mathbf{h}}) = 0.25 C_s \lambda^3 h^4 + 0.5 \Delta z \lambda h^2$$

Spherical aberration

defocus

$$+\frac{1}{6}C_{5,6}\lambda^6 k^{*6} + \frac{1}{6}C_{5,2}\lambda^6 k^{*4} k^2 + \frac{1}{6}C_{5,0}\lambda^6 k^{*3} k^3$$

$$+\ldots\}$$ -- [3740a]

The first subscript refers to the order of the coefficient in terms of real space displacement, while the secc symmetry. If the vector **k** is replaced by a complex number $\omega = \lambda k_x + i\lambda k_y$, the wave aberration function

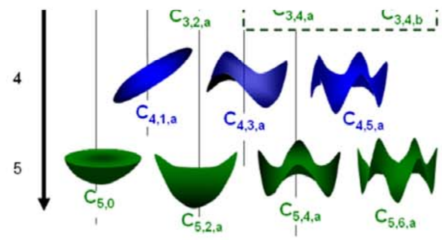

High-resolution TEM

Figure 3740 shows the aberration coefficients from 0[th] to 5[th] order.

From https://www.globalsino.com/EM/page3740.html

$$W(k) = \mathrm{Re}\{C_{0,1}\lambda k^*$$
$$+\frac{1}{2}C_{1,2}\lambda^2 k^{*2} + \frac{1}{2}C_{1,0}\lambda^2 k^* k$$
$$+\frac{1}{3}C_{2,3}\lambda^3 k^{*3} + \frac{1}{3}C_{2,1}\lambda^3 k^{*2} k$$
$$+\frac{1}{4}C_{3,4}\lambda^4 k^{*4} + \frac{1}{4}C_{3,2}\lambda^4 k^{*3} k + \frac{1}{4}C_{3,0}\lambda^4 k^{*2} k^2$$
$$+\frac{1}{5}C_{4,5}\lambda^5 k^{*5} + \frac{1}{5}C_{4,3}\lambda^5 k^{*4} k + \frac{1}{5}C_{4,1}\lambda^5 k^{*3} k^2$$
$$+\frac{1}{6}C_{5,6}\lambda^6 k^{*6} + \frac{1}{6}C_{5,2}\lambda^6 k^{*4} k^2 + \frac{1}{6}C_{5,0}\lambda^6 k^{*3} k^3$$
$$+\ldots\}$$ -- [3740a]

The first subscript refers to the order of the coefficient in terms of real space displacement, while the secc symmetry. If the vector **k** is replaced by a complex number $\omega = \lambda k_x + i\lambda k_y$, the wave aberration function

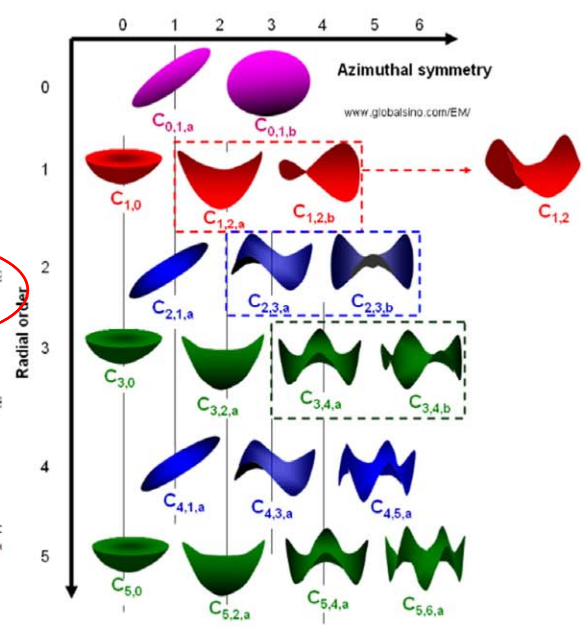

High-resolution TEM

Figure 3740 shows the aberration coefficients from 0[th] to 5[th] order.

the aberration-corrected transmission electron microscope

(Rose, 1990; Haider et al., 1998)

Maximilian Haider, Stephan Uhlemann,
Eugen Schwan, Harald Rose, Bernd Kabius, Knut Urban
NATURE, VOL 392, 1998

transfer doublet

hexapole

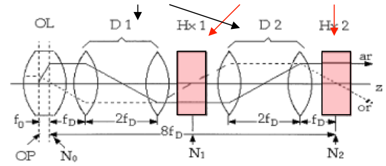

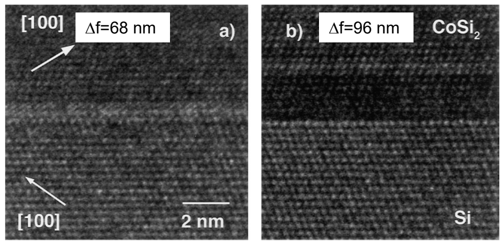

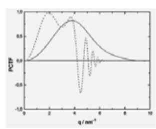

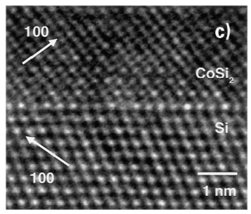

Cs-corrector

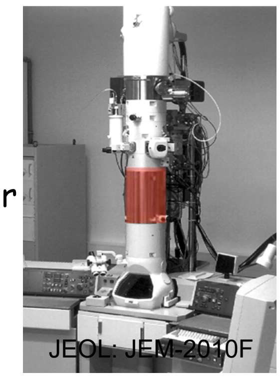

Sharp interfaces

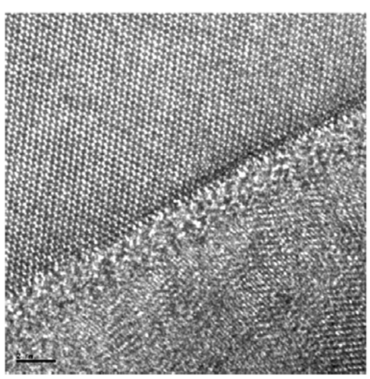

Fig. 3. TEM image of a cross section of a MOSFET transistor showing the amorphous gate oxide layer between crystalline silicon and polycrystalline silicon, recorded with monochromator on and Cs corrector on. The image was taken with 0.1 nA beam current on the CCD, 1 s exposure time, and 2 mrad half convergence angle.

No delocalisation at interfaces anymore

Cs corrector off

Cs corrector on

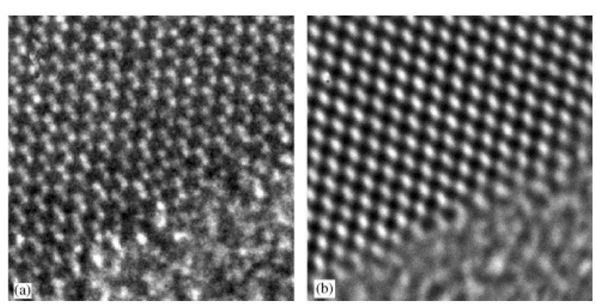

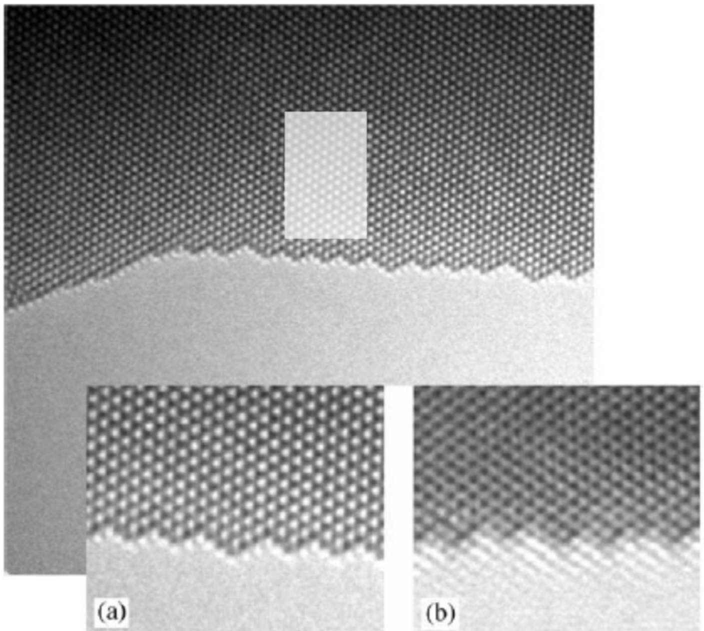

Cs corrector on (a), off (b)

Gold crystal

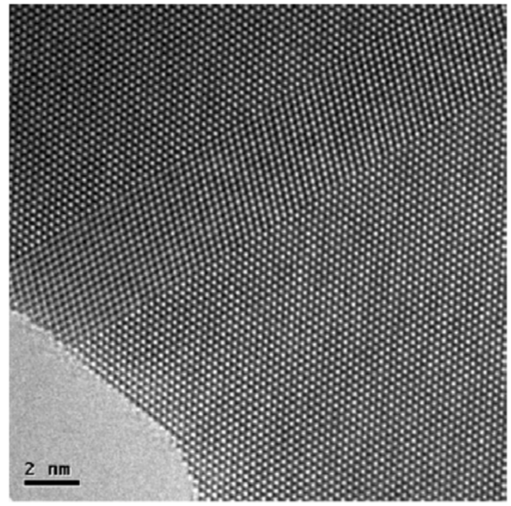

- DEMO Transfer function

Handbook of Nanoscopy, Volume 1&2

Copyright © 2012 Wiley-VCH Verlag GmbH & Co. KGaA

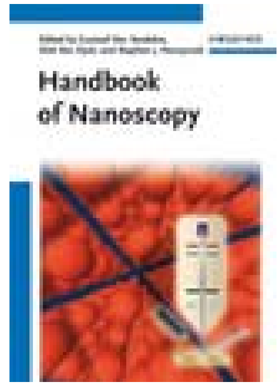

Editor(s): Gustaaf Van Tendeloo, Dirk Van Dyck, Stephen J. Pennycook
Published Online: 23 MAY 2012 05:12AM EST
Print ISBN: 9783527317066
Online ISBN: 9783527641864
DOI: 10.1002/9783527641864

3 Ultrahigh-Resolution Transmission Electron Microscopy at Negative Spherical Aberration

Knut W. Urban, Juri Barthel, Lothar Houben, Chun-Lin Jia, Markus Lentzen, Andreas Thust, and Karsten Tillmann

NCSI

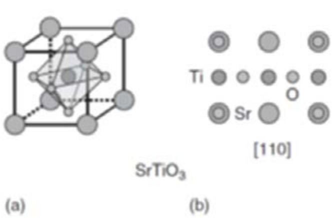

Figure 3.2 $SrTiO_3$. (a) Perspective view of the unit cell. (b) Projection along the [110] crystal direction. In this viewing direction, three types of atomic columns are distinct, which are occupied alternatively with strontium and oxygen, with titanium, and with oxygen atoms.

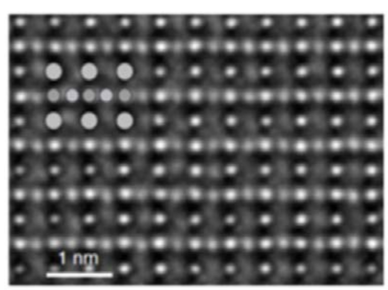

Figure 3.3 Experimental image of $SrTiO_3$ taken along the [110] zone axis employing the NCSI technique (FEI Titan 80–300 with imaging corrector, operated at 300 keV). All three atomic species are visible (compare inset) at bright contrast on a dark background.

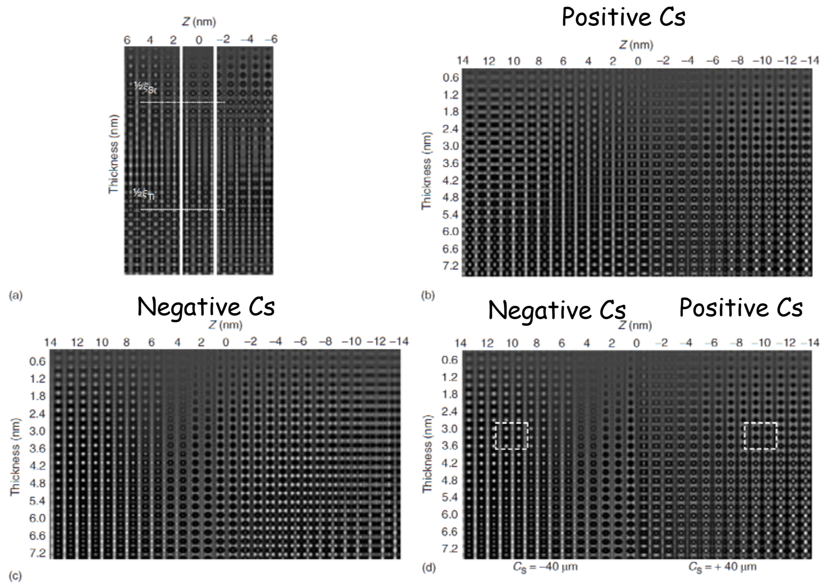

Figure 3.4 Simulated images for $SrTiO_3$ [110] at 200 keV. The composite shows a single unit cell in [110] projection for different defocus values Z and sample thicknesses at an electron energy of 200 keV for the spherical aberration parameter C_S = 0 nm, +40 µm, and −40 µm (a–c). (d) Direct comparison of the positive and negative C_S situation, where in the $-C_S$ case overfocus (positive values of Z) and in the positive C_S case the usual underfocus (negative values of Z) is applied. The frame is used as a guide for the eye for same sample thickness.

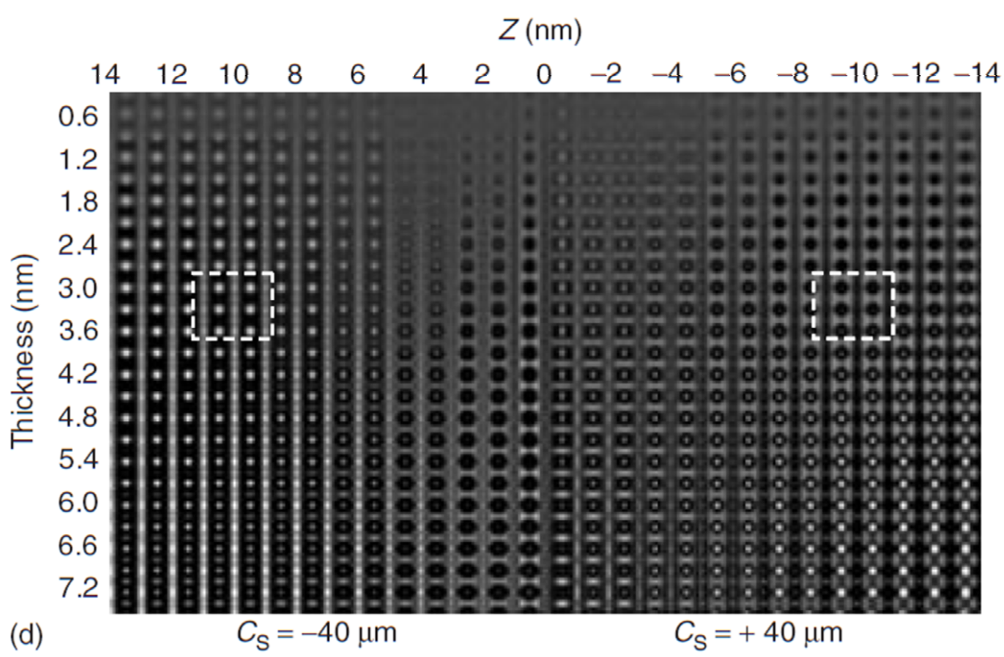

High-resolution TEM Marco Cantoni

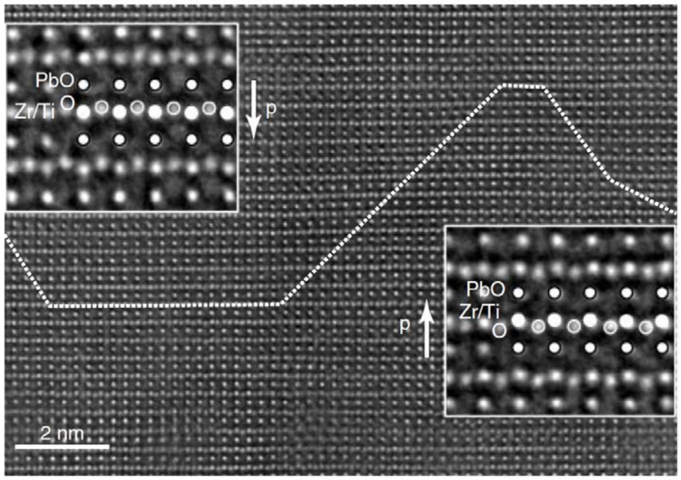

Figure 3.13 $Pb(Zr_{0.2}Ti_{0.8})O_3$ imaged along the [110] direction. The inset on the left shows that the horizontal Zr/Ti atom rows are shifted toward the respective Pb atom row above the Zr/Ti row. Oxygen is shifted even more, thus becoming no longer co-linear with the Zr/Ti rows. This indicates that the material is ferroelectrically polarized. The polarization vector **p** points downward. The inset on the right shows opposite atomic shifts. The direction of the polarization vector there is upward. The dotted line shows the appertaining ferroelectric inversion domain wall. With respect to the atomic structure, the inclined domain-wall sections consist of vertical transversal and horizontal longitudinal domain-wall segments. As a result they are uncharged. The horizontal sections are longitudinal domain walls, which are charged [56].

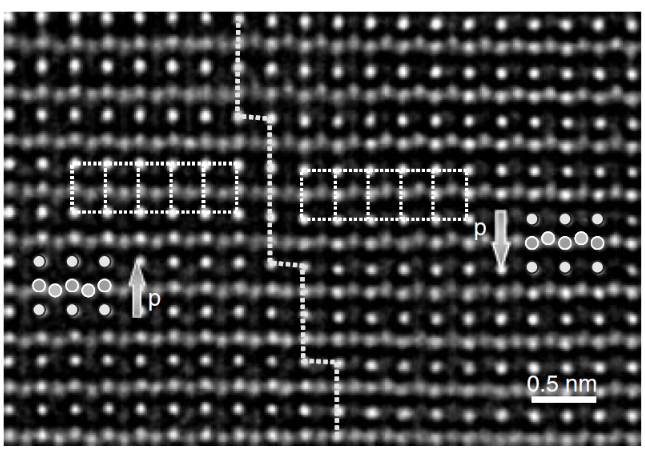

Figure 3.14 A 180° domain-wall segment of mixed type seen edge-on. The arrows "**p**" indicate the opposite polarization directions across the domain wall. The parallelograms denote the segments of transversal domain wall. The vertical dotted line marks the central plane of the domain wall. The horizontal dotted lines trace projected unit cells on either side of the domain wall. Indicated by the shift of the oxygen atoms, "up" on the left and "down" on the right of the central plane indicates directly that the width of the wall is a single <110> projected unit cell wide [56].

Cs-corrected imaging

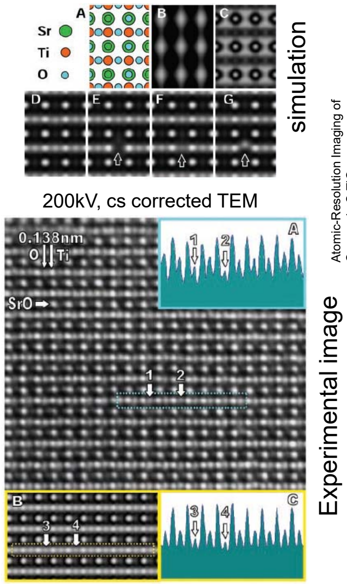

Atomic-Resolution Imaging of Oxygen in $SrTiO_3$
C. L. Jia, M. Lentzen, K. Urban
SCIENCE VOL 299 (2003)

- direct imaging of heavy and light atoms in a sinlge image
- No delocalisation: atoms are seen at their real position

Oxygen vacancies in $YBa_2Cu_3O_x$

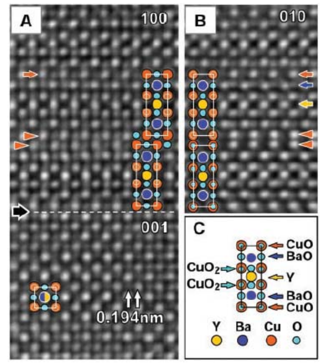

Chun-Lin Jia, Markus Lentzen, and Knut Urban
Microsc. Microanal. 10, 174–184, 2004